

Seasonal multisite low-cost sensor measurements to estimate spatial and temporal variability of particulate matter pollution in Nairobi, Kenya



Ezekiel W. Nyaga ^a, Michael R. Giordano ^{a,b,i}, Matthias Beekmann ^{a,b,*}, Daniel M. Westervelt ^{d,e}, Michael Gatari ^f, John Mungai ^g, Godwin Opinde ^h, Albert A. Presto ^{c,i}, Emilia Tjernström ^j, V. Faye McNeill ^k, R. Subramanian ^{a,b,c,1}

^a Université Paris Cité and Univ Paris Est Créteil, CNRS, LISA, F-75013, Paris, France

^b Univ Paris Est Créteil, Université Paris Cité, Ecole des Ponts et CNRS, OSU-EFLUVE UAR 3653, F-94010, Créteil, France

^c Kigali Collaborative Research Centre, Kigali, Rwanda

^d Lamont Doherty Earth Observatory of Columbia University, New York, NY, USA

^e Université Mohammed VI Polytechnic, Benguerir, Morocco

^f University of Nairobi Institute of Nuclear Science and Technology, Nairobi, Kenya

^g Innovations for Poverty Action (IPA), Nairobi, Kenya

^h Kenyatta University Department of Spatial & Environmental Planning, Nairobi, Kenya

ⁱ Department of Mechanical Engineering, Carnegie Mellon University, Pittsburgh, PA, USA

^j Centre for Development Economics and Sustainability of Monash University, Melbourne, Victoria, Australia

^k Columbia University Department of Chemical Engineering, New York, NY, USA

ABSTRACT

Ambient concentrations of fine particulate matter ($PM_{2.5}$) in sub-Saharan African cities like Nairobi can vary significantly due to the distribution and intensity of local and regional emission sources. We assess the spatiotemporal variability of $PM_{2.5}$ in Nairobi using low-cost sensor and reference instrument data from urban background (2020–2022) sites and from several source-specific sites (June to December 2021). To our knowledge, this work represents the longest and most spatially differentiated dataset for this city.

Data from urban background sites demonstrates seasonal variation driven by precipitation. $PM_{2.5}$ concentrations were higher during the warm-dry (JF, 17.1–18.8 $\mu g m^{-3}$) and cool-dry (JJAS, 21.0–25.5 $\mu g m^{-3}$) seasons and lower during the rainy seasons of MAM (14.8–17.0 $\mu g m^{-3}$) and OND (13.2–17.2 $\mu g m^{-3}$). Seasonal differences are systematic, and larger than the inter-annual variability. Our analysis of source-specific $PM_{2.5}$ measurements (June to December 2021) reveals for the more polluted JJAS season the highest $PM_{2.5}$ recorded at traffic/residential sites (28.8–29.1 $\mu g m^{-3}$), followed by urban background (23.3–24.1 $\mu g m^{-3}$) and sub-urban background (22.5 $\mu g m^{-3}$). The traffic/residential impacted sites demonstrate noticeable morning and evening peaks associated with traffic and residential emissions, while diurnal profiles for urban background and sub-urban background sites remain flat during the day but display noticeable evening peaks, pointing again to the impact of residential emissions. At the urban background site and during the JJAS season, an additional midday peak is probably related to residential cooking emissions.

1. Introduction

Sub-Saharan Africa (SSA) has undergone rapid urbanisation and economic development(Castells-Quintana and Wenban-Smith, 2020; United Nations, 2018), leading to increased anthropogenic activity and environmental degradation, including worsening air quality(Fisher et al., 2021). Most cities in this region experience elevated levels of fine particulate matter ($PM_{2.5}$, particles smaller than 2.5 μm in diameter) (Gaita et al., 2014; Okure et al., 2022; Pope et al., 2018; Subramanian et al., 2020). Exposure to high $PM_{2.5}$ levels is linked to respiratory and

cardiovascular conditions as well as decreased life expectancy(C. A. Pope and Dockery, 2006). Ambient particulate matter also seriously affects climate(Chen et al., 2021) and atmospheric visibility(Yadav et al., 2022). Atmospheric primary $PM_{2.5}$ is directly emitted from anthropogenic and natural sources while secondary $PM_{2.5}$ forms due to chemical transformations in the atmosphere(Behera and Sharma, 2010). In Nairobi, primary anthropogenic emissions mainly come from traffic (Gaita et al., 2014; Kinney et al., 2011; Pope et al., 2018), industries (Gatari et al., 2009), use of wood fuel and charcoal(Egondi et al., 2016; Manshur et al., 2023; Muindi et al., 2016; Mutahi et al., 2021), and open

* Corresponding author. Université Paris Cité and Univ Paris Est Créteil, CNRS, LISA, F-75013, Paris, France

E-mail address: matthias.beekmann@lisa.ipsl.fr (M. Beekmann).

¹ Currently at Center for Study of Science, Technology & Policy, Bengaluru, Karnataka, India 560094

burning of municipal waste(deSouza et al., 2017; Nthusi, 2017), while natural emissions include mineral dust and sea salt due to transport (Gaita et al., 2014). The intensity of PM_{2.5} within Nairobi varies depending on the distribution of emissions sources, and transport mechanisms, with elevated pollution occurring near emission sources but decreases rapidly with distance(Kinney et al., 2011). In addition, the urban background concentration is impacted by regional pollution transport(Boiyo et al., 2018; Kalisa et al., 2023; Kirago et al., 2022). To effectively assess local emissions and the influence of external pollution sources, comprehensive air quality studies in urban areas should therefore collect data from diverse locations—including sites near emissions sources, urban background sites, and background sites outside the city.

Carefully calibrated low-cost PM_{2.5} sensors offer a promising solution for expanding air quality monitoring networks in SSA, thanks to technological advancements(Jayaratne et al., 2020; Kelly et al., 2017). These sensors, which measure particle concentrations using light scattering techniques(Austin et al., 2015; Crilley et al., 2018; Ouimette et al., 2024), have been shown to capture concentration variability with sufficient accuracy for air quality assessments in the region(McFarlane et al., 2021; Njeru et al., 2024; Pope et al., 2018; Raheja et al., 2023; Subramanian et al., 2020). Unlike cities in developed countries with well-established monitoring networks, cities in SSA primarily rely on research-driven, ad-hoc measurements. The affordability of low-cost sensors makes it possible to establish denser networks, which are essential for filling the current gap in long-term air quality data. However, these sensors are prone to uncertainties and weather-related performance degradation(Ouimette et al., 2024). To ensure accuracy, sensors must be calibrated against reference-grade instruments, ideally in conditions similar to the monitoring environment(Giordano et al., 2021; Malings et al., 2019, 2020). While no standard calibration procedure exists, a range of linear regression and machine-learning models have been proven effective in correcting low-cost sensor data for air quality studies(Malings et al., 2020; McFarlane et al., 2021; Raheja et al., 2023).

The long-term variability of PM_{2.5} in Nairobi is still poorly understood, existing studies that conducted year-round measurements more than a decade ago used two monitoring stations(Gaita et al., 2014) and the most recent study used a single monitoring location(Kirago et al., 2022). The 2008–2010 study(Gaita et al., 2014) deployed filters every one or two days, while the 2019–2020 study(Kirago et al., 2022) collected filter samples weekly. Both studies reported high seasonal concentrations from June to September (JJAS), which dropped by 50 % during the wet period in October and November (ON) (Gaita et al., 2014). January and February saw elevated pollution levels due to regional dust transport. In 2009, irregular weather patterns contributed to prolonged droughts during the typically wet March to May (MAM) season, leading to unusually high pollution levels. Normally, this period records around 450 mm of rainfall, but only 223 mm fell that year.

This work contributes to the literature by providing continuous, long-term measurements of PM_{2.5} in Nairobi using a dense network of six sensors (in addition to measurements performed at the US embassy), calibrated using a reference-grade equivalent beta attenuation monitor (BAM). The BAM-collocation allows us to generate correction factors, as described in the Methods section, which address the known inaccuracies of low-cost monitors(Zou et al., 2021). Our air quality monitoring effort included continuous monitoring at three urban traffic sites, three urban background sites, and a suburban site, filling crucial gaps in existing measurements in terms of both temporal and spatial coverage. These data can inform the city's air quality management and serve as a valuable reference for future research. Given the rapid urbanisation in the region and its effects on air quality, this type of comprehensive study is increasingly urgent.

2. Methods

2.1. Study area

The study is conducted in the city of Nairobi, Kenya, located in Eastern Africa between latitude 1°17'11.0004"S and Longitude 36°49'2.0028"E at an altitude of approximately 1800m. Nairobi covers approximately 684 km² and is inhabited by over 4.2 million people. The city is typically characterised by a subtropical highlands climate with predominantly easterly winds arising from the north-south intertropical convergence zone drift (ITCZ). The winds drive moisture inflow from the Indian Ocean, resulting in wet periods that cover March, April and May (MAM) and October, November, and December (OND), while the dry periods span January, February (JF) and June, July, August, September (JJAS) season(Henne et al., 2008).

2.2. Field deployment and site characteristics

Our data collection, detailed in Table 1, ran between January 2020 to December 2022 (Fig. 1). Our original plan to deploy the sensor nodes across schools in Nairobi was disrupted by lockdowns, curfews, and school closures due to the COVID-19 pandemic. As a result, the sensors remained collocated at an urban background site on a low-rise building at the Innovations for Poverty Action (IPA) offices in Nairobi's Westlands neighbourhoods throughout 2020, but no reference instrument was present. This provided an extended period during which we can compare sensor measurements at a single location. The reference instrument was only made available in April 2021 at the University of Nairobi (UoN), where four sensors were co-located from April 1 to May 31, 2021, to provide calibration measurements. Then, between June and December 2021, sensors were redeployed to new sites that were chosen to cover a range of source profiles, including traffic, traffic/residential, urban background, and suburban background sites.

The sensors were mounted on the fourth-floor rooftops at the University of Nairobi and KUCC sites. In the other sites, however, the sensors were installed on the roofs of single-story homes. At the UoN urban background site, we installed the sensors at an existing air quality station located on the rooftop of the School of Engineering, roughly 20 m from Harry Thuku Drive, a low-traffic road. Additional measurements came from a BAM at the US embassy in Gigiri, a low-density neighborhood around 6 km north of Nairobi Central Business District (CBD). We deployed two sensors on the Kenyatta University City Campus (KUCC), a high-traffic site within the CBD, only 200m from the intersection of two major traffic motorways, Haile Selassie and Uhuru Highway. Another traffic site, Marurui, is located around 9 km northwest of the CBD and less than 50 m from another major motorway, the Northern Bypass Road, where heavy trucks were frequently re-routed to avoid city

Table 1

Low-cost sensors measurement locations, location type, and duration of measurements.

Site name	Site code	Site classification	Measurement duration
Kenyatta University City Campus	KUCC	traffic	2021-06-01 2021-12-31
Buruburu	Buruburu	traffic/ residential	2021-06-01 2021-12-31
Marurui	Marurui	traffic/ residential	2021-06-01 2021-12-31
University of Nairobi	UoN	urban background	2021-04-01 2021-12-31
IPA offices Nairobi	IPA	urban background	2020-01-15 2021-12-31
US embassy Nairobi	US Embassy	urban background	2022-01-01 2022-12-31
Ngong	Ngong	suburban	2021-06-01 2021-12-31

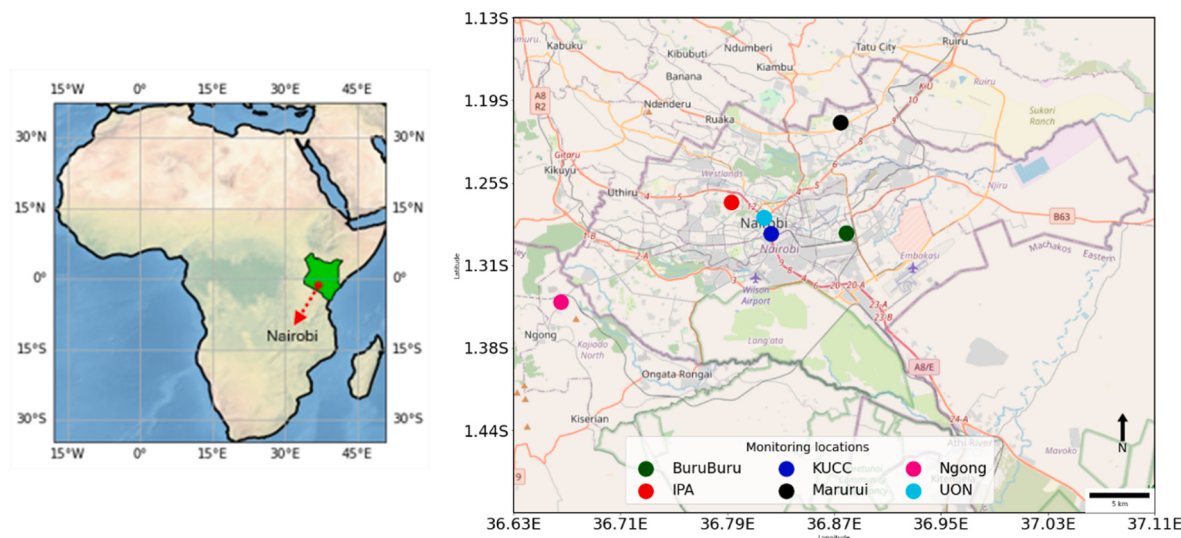


Fig. 1. (a) Map of Africa showing the location of Kenya in eastern Africa and the city of Nairobi, (b) Satellite map of Nairobi showing the measurement locations used in this study. Maps are generated using Cartopy, a cartographic Python library(Elson et al., 2018).

congestion. This site allows us to assess the impact of truck-dominated traffic on air quality, relative to the car-dominant traffic in the CBD. Our last traffic site, BuruBuru, was located approximately 7 km east of the CBD. Both Marurui and BuruBuru are in densely populated areas, allowing us to detect the influence of joint traffic and residential emissions. Finally, Ngong, a suburban residential area some 20 km southwest of the CBD serves as a suburban monitoring site. We use PM_{2.5} data from a single low-cost sensor at each site, except for IPA and UON, where it was obtained by averaging the data from eight and two sensor units, respectively.

2.3. Instrumentation

We use sensor nodes developed by Clarity Movement Corporation (Miech et al., 2021; Zaidan et al., 2020). The device contains a Plan-tower PMS6003 sensor to monitor fine particulate matter concentrations in addition to relative humidity and temperature measurements(Miech et al., 2021; Quimette et al., 2024). The sensor nodes are solar-powered, transmitting data using a cellular connection to the Clarity cloud for storage(Gonzalez et al., 2019; Zaidan et al., 2020). The sensors measure fine particulate matter through laser light scattering technology. A Met One Beta Attenuation Monitor 1020 (BAM) provided the reference measurements for sensor calibration(Gobeli et al., 2008). The BAM uses beta-ray attenuation to estimate the mass of PM_{2.5} collected on a filter tape(Gobeli et al., 2008).

2.4. Calibration

The BAM and fine particulate matter (PM) sensors were deployed together for two months, from April 1 to May 31, 2021 at the UoN site. Hourly PM_{2.5} data from BAM and PM_{2.5}, relative humidity, and temperature data from PM sensors were merged into a common dataset. We then performed quality control checks to exclude anomalous observations from this dataset. A multi-linear regression model was developed for one “golden sensor” in this collocation following the low-cost PM sensor calibration best practices recommended by Giordano et al. (2021) and procedures outlined in previous research (Malings et al., 2020; Si et al., 2020). BAM data were randomly split into two subsets, 70 % and 30 %, for model training and validation, respectively. The MLR model used raw PM_{2.5} concentrations [in $\mu\text{g m}^{-3}$] and relative humidity [in %]. The following equation illustrates the structure of our model:

$$\text{PM}^{\text{corrected}} = (0.6251 \pm 0.009)\text{PM}^{\text{sensor}} - (0.226 \pm 0.008)\text{RH}^{\text{sensor}} + 19.454$$

$\text{PM}^{\text{corrected}}$ represents corrected sensor measurements, $\text{PM}^{\text{sensor}}$ represents raw sensor measurement, and $\text{RH}^{\text{sensor}}$ denotes relative humidity from the sensor. We calculate statistical metrics to describe the relationship between the post-calibrated sensor unit and the BAM from 5 fold cross-validation procedure: Pearson correlation $r = 0.88$, RMSE ($0.45 \mu\text{g m}^{-3}$), and MBE ($0.17 \mu\text{g m}^{-3}$). After the calibration model was developed for the “golden sensor”, the other sensor responses were corrected for slope and bias relative to this sensor based on the collocation at the calibration site, and then the calibration model was applied to this corrected dataset.

3. Results and discussion

3.1. Day-to-day variability in urban background concentrations of fine particulate matter

We present an evaluation of the day-to-day and seasonal variability of the 3-year (2020–2022) PM_{2.5} mass concentrations measured at urban background sites, namely the IPA and US embassy in Nairobi. We first evaluate the suitability of considering the two sites as similar enough to combine them into a single time series(Fig SI 1). Between October and December 2021, we find a strong correlation coefficient ($r = 0.88$) while the US Embassy has a mean bias error of $-2.85 \mu\text{g m}^{-3}$ with respect to IPA site. We prefer here showing the original US embassy data, but keep in mind differences to IPA in the discussion of the interannual variability.

The daily average PM concentrations in Fig. 2 display comparable trends for corresponding periods with severe pollution during dry months in JJAS and JF, marked by high and frequent concentration spikes. The major spikes from these sites agree reasonably well but tend to be higher at IPA (2020, 2021, $40\text{--}50 \mu\text{g m}^{-3}$) compared to US embassy (2022, $<30 \mu\text{g m}^{-3}$). Several prominent pollution episodes were persistent between August and September 2020 and 2021, suggesting possible regional transport since the predominant air masses over Nairobi (calculated with the Hysplit back trajectory model, see figure SI 2) originate from Tanzania (south of Nairobi), which is reported to experience rampant biomass burning with high aerosol optical depth (AOD) during the months of JJAS(Boiyo et al., 2018; Kalisa et al., 2023; Kirago et al., 2022). During the three years, the minimum, mean, and maximum concentrations were 4.8, 18.3 and $52.5 \mu\text{g m}^{-3}$, respectively.

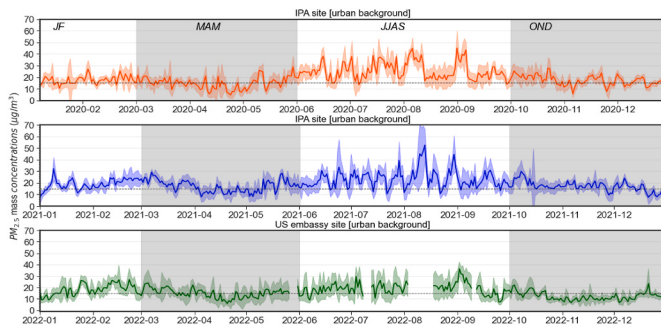


Fig. 2. Shows daily averages in PM_{2.5} mass concentrations in the years 2020 (top), 2021 (middle), and 2022 (bottom) at the IPA site (2020–2021) and the US embassy (2022). The shaded areas represent the 95 % confidence interval of the daily average values. The standard deviation values are calculated from the hourly PM_{2.5} concentrations. The months of JF represent the warm-dry season, MAM the long-wet season, JJAS the cool-dry season, and OND the short-wet season. The dashed lines at 15 $\mu\text{g m}^{-3}$ indicate the WHO air quality guideline for daily average PM_{2.5} concentrations.

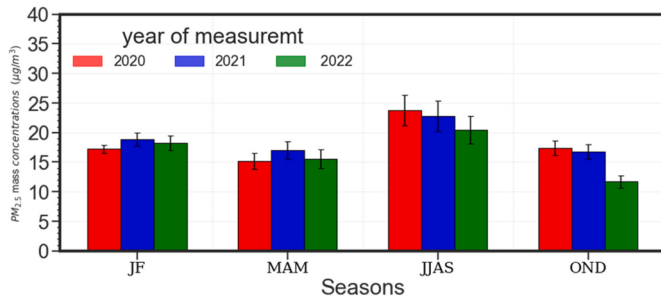


Fig. 3. Shows average seasonal concentrations of PM_{2.5} (mean, and standard deviation of the mean [$\mu\text{g m}^{-3}$]) at IPA (2020–2021) and US embassy (2022) monitoring locations.

Noteworthy, this annual average concentration was three times higher compared to the World Health Organization's (WHO) annual average guideline of 2021 (5 $\mu\text{g m}^{-3}$) (WHO, 2021). It was 19.5, 19.4, and 16.0 $\mu\text{g m}^{-3}$ in 2020, 2021, and 2022, respectively. Interestingly, the 3 $\mu\text{g m}^{-3}$ lower annual average at the US embassy in 2022, with respect to the

IPA site in 2020, and 2020 is nearly entirely explained by the 3 $\mu\text{g m}^{-3}$ bias of US embassy with respect to IPA site during the common measurement period. Thus, the corrected annual averages would be very similar. The WHO daily average PM_{2.5} threshold of 15 $\mu\text{g m}^{-3}$ was exceeded for most of the days in 2020 (262 days), 2021 (281 days), and 2022 (179 days).

3.2. Seasonal variability at urban background sites

Next, we analyse the seasonal variations of urban background concentrations in Nairobi. We follow a broad definition of biannual wet and dry seasonal cycles for tropical regions: a warm-dry season that includes January and February (JF), followed by a long-wet season from March to May (MAM), a cool-dry season from June to September (JJAS) and a short-wet season from October and December (OND) (Yang et al., 2015). We first analyse the seasonal precipitation and temperature variations, as calculated from meteorological data taken at the Jomo Kenyatta International Airport (Fig. 4b). Precipitation ranged from 53.6 to 70.2 mm in JF, 36.4–139.1 mm in MAM, 9.7–58.4 mm in JJAS, and 13.2–123.0 mm in OND. The average monthly temperature shifts to a limited extent, about 4 °C, with the hottest months being February and March (21–22 °C) and the coolest July and August (17–18 °C). The air masses arriving in Nairobi between December and February originate from the northeast but span south to the southeast between March and November (Kirago et al., 2022). From the point of view of precipitation, this climatological seasonal cycle has been well followed from 2020 to 2022. Nevertheless, the seasons appear to shift roughly by one month with respect to the definition described earlier in this work. Therefore, the driest months extend from July to October (instead of June to September), and the rainiest ones from April to June (instead of March to May). However, as these precipitation data are local, we stick to the general definition of seasons described above (Fig. 3).

With respect to Figs. 2 and 3 and Table SI 1, the day-to-day variability in PM_{2.5} is larger in dry (JF and JJAS) seasons than in wet seasons (MAM and OND). This seasonal variation is robust from one year to the other. Furthermore, differences between the seasons are generally more significant than between the years. The only consistent trend is seen during the JJAS seasons, which shows a gradual decrease from 2020 to 2022 but remains the most polluted season in all three years (in the sense that concentrations decreased for two consecutive years). As noted earlier, PM_{2.5} concentration enhancement during the JJAS season could arise from regional transport from the southerly directions (Tanzania,

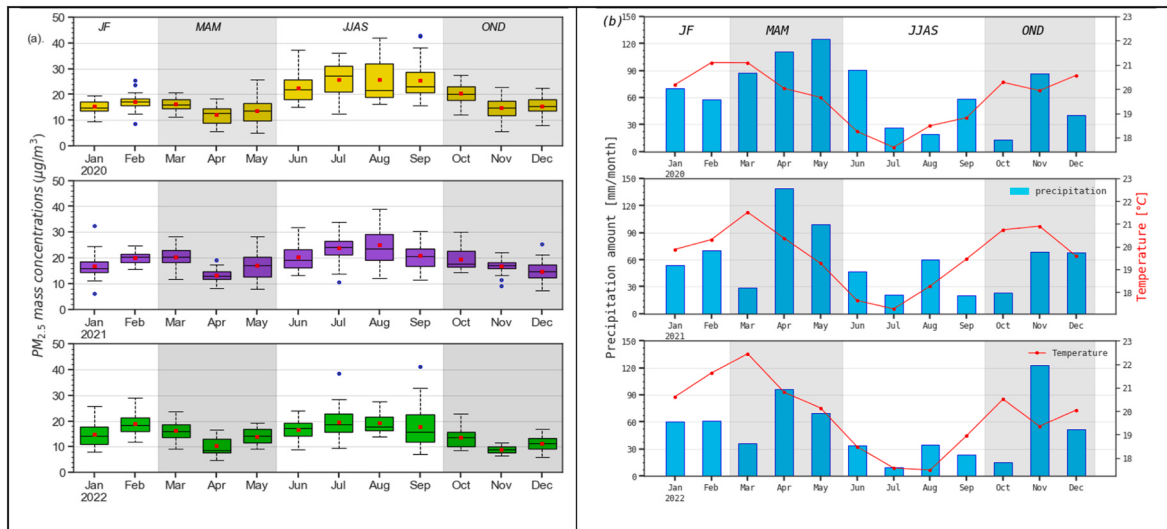


Fig. 4. (a) Displays monthly boxplots of 24-h average PM_{2.5} concentrations, (b) corresponding monthly precipitation and temperature measured at the Jomo Kenyatta International Airport. Bar plots in light blue show the monthly precipitation amounts, and the red line shows the monthly average temperature. Hourly precipitation and temperature were downloaded from National Oceanic and Atmospheric Administration (NOAA), Integrated Surface Database (ISD) (NCEI, 2024).

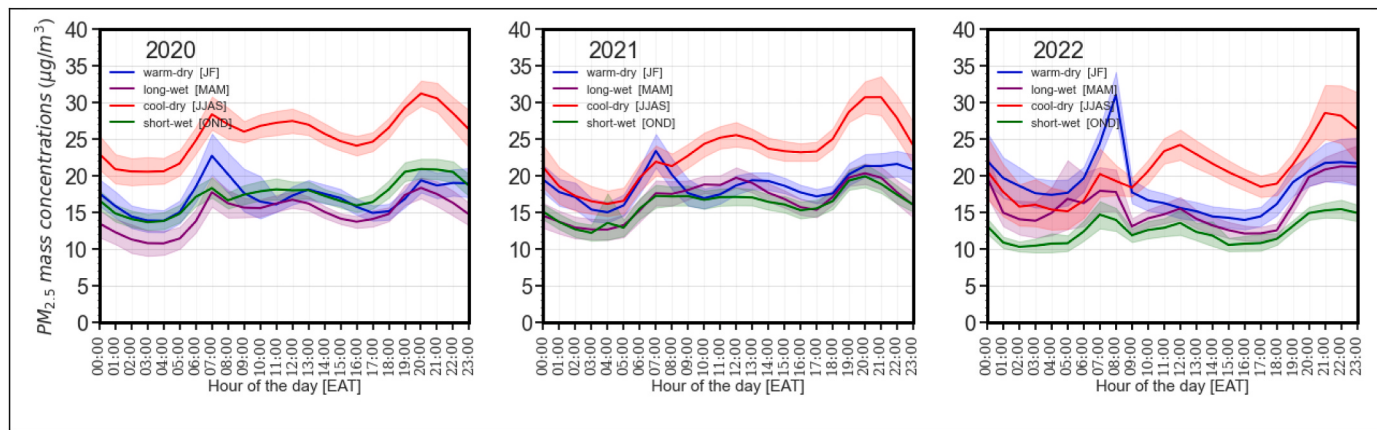


Fig. 5. Diurnal variations of seasonal PM_{2.5} concentrations at IPA (2020–2021) and US embassy (2022) urban background locations. The shaded areas show the 95 % confidence interval of the hourly average values.

Madagascar) due to biomass burning during this period(Kalisa et al., 2023). The seasonal cycles of PM_{2.5} concentrations reported in previous studies show reasonable agreement with our work(Gaita et al., 2014). Although this comprehensive seasonal evaluation was presented more than a decade ago (2008–2010), it reported heavy pollution loading during JJAS ($25 \pm 8.6 \mu\text{g m}^{-3}$), while the cleanest air was observed in ON ($8.9 \pm 2.4 \mu\text{g m}^{-3}$) (Gaita et al., 2014), which is consistent with our findings.

The study also coincided with the global outbreak of the COVID-19 virus in 2020. When the first case of the virus was reported in Nairobi on March 10, 2020, various preventive measures were implemented, including nighttime curfews and cessation of movement into and outside the county of Nairobi, except for essential service providers. Assessment of the effects of these measures on air pollution was beyond the scope of this study since our monitoring was only limited to a single urban background location (IPA offices in Westlands, Nairobi), which began in January 2020. However, it is worth noting that during the lockdown period, road transport dropped significantly while residential activities increased; these factors could generate opposite effects on air pollution. As shown in Figures 3 and 4 seasonal averages do not show any clear tendency in 2020 with respect to the other years.

3.3. Seasonal-dependent diurnal profiles

The diurnal profiles from the two urban background sites show an interesting general structure, with low night-time PM concentrations (minimum between 02:00 and 05:00 a.m. EAT) and an interesting season-dependent pattern characterised by a threefold peak profile, with peaks during morning, noon, and evening hours (Fig. 5). Morning peaks between 07:00 and 08:00 a.m. EAT are only important during the warm-dry (JF) season. For the other seasons, the peaks often correspond to the shoulders of a larger peak that emerges during noontime. The peaks occurring around 12:00 p.m. EAT are most apparent during the cool-dry

season. Evening peaks are evidently largest around 09:00 p.m. EAT except during warm-dry seasons when they extend up to 11:00 p.m. EAT. The observed diurnal patterns are typically similar during the three years, although the magnitude of their peaks tends to be different. These diurnal profiles have been linked to the influence of the daily cycle of activities and the evolution of planetary boundary layer height (PBLH) (Pope et al., 2018). Morning and evening concentration peaks have been linked to an increase in anthropogenic activities, including traffic and the burning of wood fuels, kerosene, and charcoal in households (Manshur et al., 2023; Muindi et al., 2016). The midday peak is interesting and not previously observed in other places in East Africa. Its presence is poorly understood since it corresponds to the period when atmospheric boundary layer height is well developed, and local emissions are expected to be most diluted. An assessment of indoor air quality between October and December 2020 in the informal settlements of Kibera in Nairobi reported three concentration peaks of PM_{2.5} diurnal profile during the early morning ($10 \mu\text{g m}^{-3}$), late morning ($55 \mu\text{g m}^{-3}$) and an evening peak ($30 \mu\text{g m}^{-3}$) (Manshur et al., 2023). Interestingly, the afternoon one was the largest, signifying the importance of residential emissions during this hour(Manshur et al., 2023). Another similar study from the informal settlements of Korogocho in Nairobi showed similar evening and late morning peaks(Muindi et al., 2016), implying the importance of residential emissions to ambient concentrations. In both studies, the primary household energy sources constituted wood fuel, charcoal and kerosene(Manshur et al., 2023; Muindi et al., 2016). Also, daytime chemistry that actively happens during noon time causes the formation of secondary aerosols, which, in addition to the entry of particles advected to ground level in well-developed PBLH conditions, can possibly lead to the development of a third-afternoon peak.

The Observation-Based Method (OBM) has been used to estimate regional and local pollution contributions (Subramanian et al., 2020). This method determines the seasonal average regional contribution by

Table 2
Statistics of daily average PM_{2.5} concentrations from June to December 2021 across Nairobi monitoring sites.

class	Location	JJAS season			OND season		
		mean $\pm \sigma_{\text{mean}}$ ($\mu\text{g m}^{-3}$)	min ($\mu\text{g m}^{-3}$)	max ($\mu\text{g m}^{-3}$)	mean $\pm \sigma_{\text{mean}}$ ($\mu\text{g m}^{-3}$)	min ($\mu\text{g m}^{-3}$)	max ($\mu\text{g m}^{-3}$)
Urban traffic/traffic/residential	KUCC	29.0 ± 0.6	14.4	52.5	26.1 ± 0.4	15.4	38.4
	Buruburu	28.8 ± 0.8	8.9	59.1	21.5 ± 0.5	8.1	35.5
	Maruri	29.1 ± 0.7	15.1	62.3	23.0 ± 0.5	10.4	45.3
Urban background	UON	24.1 ± 0.6	12.8	42.8	18.7 ± 0.4	9.3	31.6
	IPA	23.3 ± 0.6	10.4	52.5	17.1 ± 0.4	8.0	29.9
Suburban	US Embassy				14.1 ± 0.7	5.0	51.0
	Ngong	22.5 ± 0.5	10.2	40.8	16.3 ± 0.5	6.0	31.1

* σ_{mean} , max and min represent the standard deviation of the mean, maximum and minimum concentration, respectively.

calculating the minimum value of a seasonal diurnal profile from hourly measurements. The local contribution is then estimated as the difference between the ambient PM_{2.5} levels and the regional contribution. During the dry season, the regional background is expected to be more significant due to reduced rain, which limits the washout of transported pollution. However, distinguishing the urban enhancement from the regional background may be challenging (Lenschow, 2001; Zimmerman et al., 2020), suggesting that further studies, such as those using an Aerosol Chemical Speciation Monitor (ACSM), may be needed (Panda et al., 2025).

3.4. Citywide patterns in PM_{2.5} concentrations (June–December 2021)

The daily averaged PM_{2.5} concentrations calculated for JJAS season ranged from 28.8 ± 0.8 to $29.0 \pm 0.7 \mu\text{g m}^{-3}$ in traffic and traffic/residential sites (KUCC, Marurui, BuruBuru) and from 23.3 ± 0.6 to $24.1 \pm 0.6 \mu\text{g m}^{-3}$ in urban-background sites (UON, IPA, US embassy), and $22.5 \pm 0.5 \mu\text{g m}^{-3}$ at the single suburban site (Ngong). During OND season, PM_{2.5} concentrations ranged from 21.5 ± 0.5 to $26.1 \pm 0.4 \mu\text{g m}^{-3}$ at the traffic and traffic/residential sites, 14.1 ± 0.7 to $18.7 \pm 0.4 \mu\text{g m}^{-3}$ at urban-background sites, and it was $16.3 \pm 0.5 \mu\text{g m}^{-3}$ at the suburban site. Thus traffic/residential sites display about 3–12 $\mu\text{g m}^{-3}$ larger

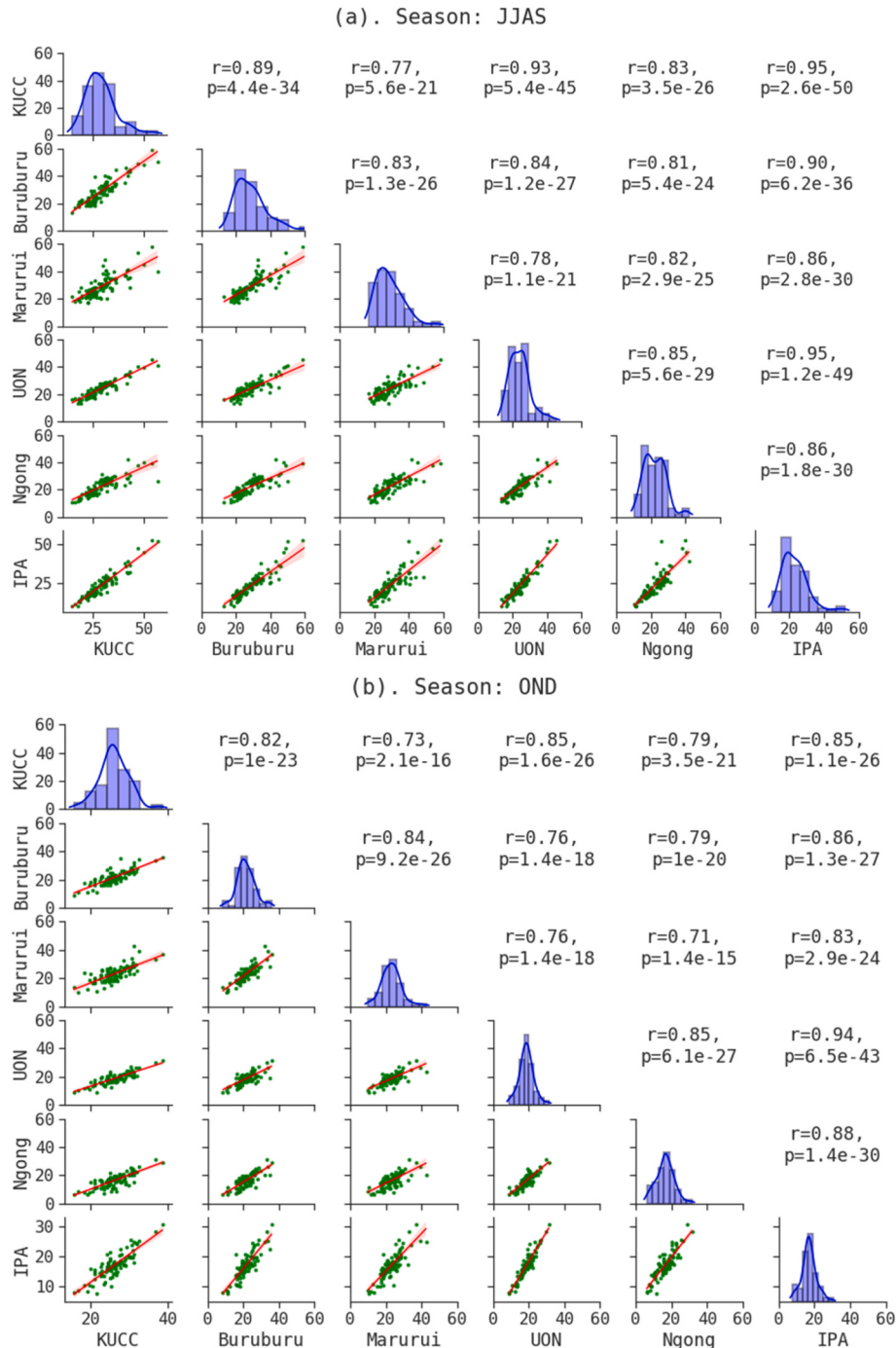


Fig. 6. Pairwise correlation between the study sites calculated from daily average PM_{2.5} concentrations for (a) JJAS and (b) OND seasons in 2021. The diagonal shows concentration distribution plots for individual sites. The corresponding upper-right section shows each subplot's correlation coefficient (r) and p-value. Concentrations are given in $\mu\text{g m}^{-3}$.

$\text{PM}_{2.5}$ levels than urban background sites, which highlights the importance of local $\text{PM}_{2.5}$ sources. First, the drop in average concentrations from the cool-dry JJAS to the rainier OND season, which was already observed for the urban background IPA and US embassy sites, also appears at the source-affected sites (KUCC, Buruburu, Marurui) and for the sub-urban Ngong site. Second, as expected, the daily average maxima for sites classified as traffic or traffic/residential range from 52.5 to 62.3 $\mu\text{g m}^{-3}$, as compared to 40.8–52.5 $\mu\text{g m}^{-3}$ for urban background and sub-urban sites.

We performed a statistical *t*-test analysis at a 95 % confidence level to determine whether the differences observed across various sites were statistically significant. The test was performed between pairs of sites with similar characteristics, referred to here as homogeneous classification (traffic/traffic, urban-background/urban-background) and dissimilar classification, referred here as heterogeneous (traffic/urban background, traffic/suburban, urban background/suburban). During the OND season, the test registered significant differences for both homogeneous and heterogeneous pairs of sites. On the contrary, for the JJAS season, only dissimilar pairs of sites reported statistically significant differences. When regional contributions drop during the wet season (OND), hyperlocal emissions may dominate, and even similar site types may show statistically significant differences. This indicates that dense air quality monitoring networks are needed to capture such site-specific differences.

Fig. 6 shows variability in $\text{PM}_{2.5}$ concentrations between monitoring sites and across the two campaign seasons. Better correlations are found between traffic sites vs urban background and suburban sites compared to traffic vs traffic sites. Correlations are generally fairly strong both in the JJAS ($r = 0.77$ – 0.95) and in the OND season ($r = 0.71$ – 0.94), meaning that atmospheric processes such as pollutant transport and dispersion affect all sites in a similar way. The detailed descriptive statistics of concentration means, minima and maxima during the seven-month city-wide measurement campaign are presented in Table 2 and Figure SI 2. The temporal variations of $\text{PM}_{2.5}$ in Fig. 7 show a common citywide trend in concentrations associated with major spikes during cool-dry months (June to September) but weakens during wet months (October to December). Mostly, the peaks tend to be detected simultaneously across all sites but with higher magnitudes at traffic sites compared to the urban background and suburban sites. This behaviour could be caused by either city-wide emission sources modulated to concentrations by similar city-wide meteorological conditions or by long-range transport affecting all sites in a similar manner. Strong precipitation events highlighted in Fig. 7 in June (17th to 21st), August (22nd to 26th) and from 24th November to 8th December apparently led to a significant drop in ambient concentrations due to the wet deposition.

The citywide differences in $\text{PM}_{2.5}$ concentrations are strongly linked to variability in the intensity of local emissions sources and precipitation

(Gaita et al., 2014; Kinney et al., 2011; Pope et al., 2018). The colder JJAS period is characterised by increased burning of wood fuels and charcoal for warming, especially within informal neighbourhoods, thus causing high residential emissions (Muindi et al., 2016). During a recent campaign that conducted one week-long (June 2019) measurements of volatile organic compounds (VOCs) in Nairobi CDB, aromatic hydrocarbons benzene and toluene were established among the most abundant VOCs (Cordell et al., 2021). These compounds play a significant role in the formation of secondary organic aerosols.

3.5. Citywide diurnal characteristics of $\text{PM}_{2.5}$ concentrations: June–December 2021

The diurnal variations of $\text{PM}_{2.5}$ mass concentrations in the JJAS and OND seasons are presented in Fig. 8. During the JJAS season, the traffic sites (KUCC, Buruburu, Marurui) display diurnal patterns with distinct morning and evening peaks that imitate the daily traffic cycles. The lowest concentrations occur between 02:00 and 04:00 a.m. EAT, coinciding with the period when minimal anthropogenic emissions and a contracted PBLH are expected. Concentrations increase sharply from 05:00 a.m. EAT and lead to morning peaks between 06:00 and 09:00 a.m. EAT. A period of concentration drop follows, starting from mid-morning to late afternoon hours, due to daytime dilution caused by the expansion of PBLH. The enhanced evening peaks at the traffic sites (KUCC, Buruburu, Marurui) have been attributed to emissions caused by the evening traffic rush and household cooking (Pope et al., 2018). The traffic/residential sites reached concentrations ranging from 31 to 44 $\mu\text{g m}^{-3}$ during the evening peaks, which surpassed their corresponding morning peaks. The prolonged morning peak at Marurui could probably be attributed to strong emissions from heavy machinery and trucks that operated throughout the day (08:00 a.m. to 05:00 p.m. EAT) in a nearby quarry during our campaign. The urban background and suburban sites experienced a single major peak between 07:00 and 09:00 p.m. EAT, during which $\text{PM}_{2.5}$ concentrations are higher by 28 %–37 % than the average daytime (06:00 a.m. to 05:00 p.m. EAT) concentrations. Although these sites missed distinct morning peaks, their profiles increased continuously until about 10:00 p.m. EAT, when a plateau was reached. The transition from JJAS to OND season is marked by a sharp fall in concentrations across all sites, mainly due to wet deposition since OND is a typical rainy period. Interestingly, the morning peak at KUCC at 06:00 a.m. EAT shows the opposite behaviour and even increases from JJAS to OND to nearly 40 $\mu\text{g m}^{-3}$. This could point to a rather local pollution impact of this site since it is situated in downtown Nairobi along busy traffic routes with high traffic emission intensity.

4. Conclusions and discussion

Our study provides a comprehensive assessment of the spatio-temporal variability of $\text{PM}_{2.5}$ concentrations across Nairobi, Kenya, leveraging data from urban background sites (2020–2022) and several source-specific sites (June to December 2021). Using carefully calibrated low-cost sensors, we describe air quality patterns that offer new insights into how pollution varies across the city. Our work sheds light on seasonal trends and the influence of specific pollution sources, contributing to our understanding of Nairobi's air quality dynamics.

At the urban background sites, we observed a clear seasonal variation, with lower $\text{PM}_{2.5}$ concentrations during the rainy seasons (OND, MAM) and higher concentrations during the dry seasons (JF, JJAS). We report lower inter-annual variability than seasonal variations. Inter-annual variability did not appear to be influenced by the mobility restrictions during the peak of the COVID-19 pandemic. The annual mean $\text{PM}_{2.5}$ across the three years of our data, 18.3 $\mu\text{g m}^{-3}$, is well in excess of the WHO threshold of 5.0 $\mu\text{g m}^{-3}$. Similarly, the daily averages from our seven-month measurements at seven different sites exceed the 15.0 $\mu\text{g m}^{-3}$ WHO threshold on most days. The seasonal diurnal variations at our urban background sites revealed a three-fold peak structure (morning,

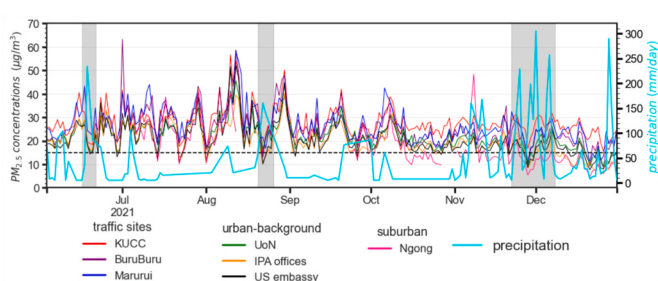


Fig. 7. Temporal variability in daily average $\text{PM}_{2.5}$ concentrations for traffic, urban background, and suburban sites within the Nairobi metropolitan area. The corresponding precipitation measurements obtained from Jomo Kenyatta International Airport are also presented. Periods with high precipitation are highlighted in grey. The 15 $\mu\text{g m}^{-3}$ lines indicate the WHO air quality guideline for daily average $\text{PM}_{2.5}$ concentrations.

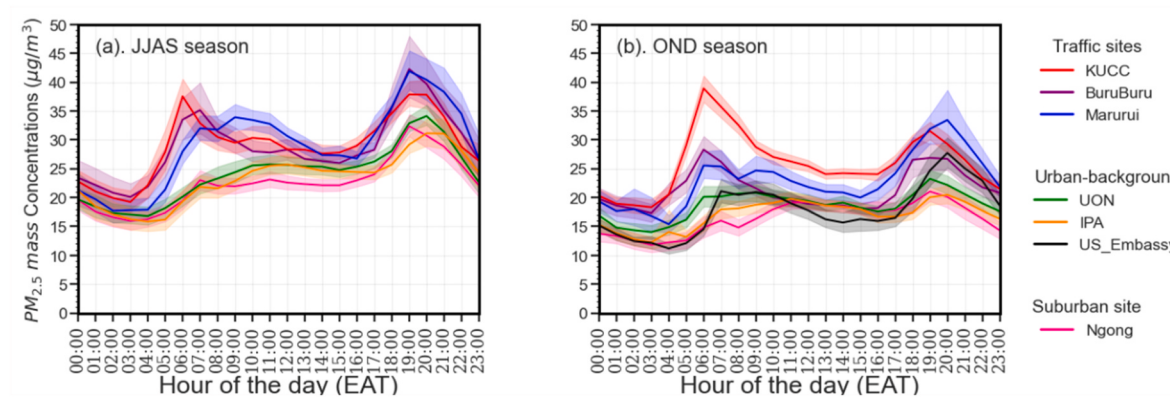


Fig. 8. Durnal PM_{2.5} variation across the study sites for (a) JJAS and (b) OND seasons with shaded areas indicating the 95 % confidence interval of the hourly average values.

noon, and evening), with the morning peak sometimes appearing only as a shoulder of the midday peak. This pattern is not fully explained by the available data, but residential emissions—particularly from cooking—may be contributing to both evening and daytime peaks, while morning rush-hour traffic peaks may be less important for these sites.

Our analysis of PM_{2.5} highlights the role of traffic emissions in morning pollution peaks at the traffic site. For mixed traffic/residential sites, the timing of evening peaks suggests that residential emissions are a key factor: evening emissions peak around 9 p.m., well after the evening traffic rush hour of 6–8 p.m. The impact of these local sources is also documented by the fact that seasonal average PM_{2.5} concentrations (June to December 2021) drop from traffic/residential-related, to urban background, and finally to suburban sites. The citywide PM_{2.5} measurements reveal that the average difference between traffic/residential and urban background concentration is 6.0 $\mu\text{g m}^{-3}$ for the JJAS season and 7.0 $\mu\text{g m}^{-3}$ for the OND season.

In addition, regional pollution advection also could influence urban Nairobi PM_{2.5} levels, although the absence of a rural background site upwind from the city limits our ability to quantify this contribution. Dust, likely from regional sources, is known to affect ambient PM_{2.5} in Nairobi (Gaita et al., 2014). Additionally, biomass burning emissions from Tanzania could reach Nairobi during the JJAS season via advection from the southerly air masses (Kalisa et al., 2023; Kirago et al., 2022). The high correlation (0.81) in daily PM_{2.5} concentrations between source-specific and background sites supports the idea of a shared local source, though common temporal variability of pollutant emissions and dispersion patterns may also contribute to this correlation.

Future research could contribute additional insights into PM_{2.5} sources through speciated PM and correlative gas-phase measurements, such as NOx as a tracer for traffic emissions. Our urban data set will be valuable for air quality model evaluation. These models, in turn, could help distinguish between local and regional sources and primary versus secondary origins of particulate matter in the Nairobi area.

CRediT authorship contribution statement

Ezekiel W. Nyaga: Writing – original draft, Visualization, Software, Methodology, Investigation, Formal analysis, Data curation, Conceptualization. **Michael R. Giordano:** Writing – review & editing, Software, Methodology, Investigation, Data curation, Conceptualization. **Matthias Beekmann:** Writing – review & editing, Supervision, Resources, Investigation, Funding acquisition, Conceptualization. **Daniel M. Westervelt:** Writing – review & editing, Resources, Conceptualization. **Michael Gatari:** Writing – review & editing, Resources, Conceptualization. **John Mungai:** Resources, Conceptualization, Data acquisition. **Godwin Opinde:** Writing – review & editing, Investigation. **Albert A. Presto:** Writing – review & editing, Resources, Conceptualization. **Emilia Tjernström:** Writing – review & editing, Resources,

Methodology, Conceptualization. **V. Faye McNeill:** Resources, Conceptualization, Resources acquisition. **R. Subramanian:** Writing – review & editing, Resources, Project administration, Methodology, Funding acquisition, Conceptualization.

Declaration of competing interest

The authors declare that they have no known competing financial interests or personal relationships that could have appeared to influence the work reported in this paper.

Acknowledgement

This work has benefited from State funding managed by the Agence Nationale de la Recherche (ANR) under the “Programme d’Investissements d’Avenir” integrated into France 2030, under the reference ANR-18-MPGA-0011. The authors also acknowledge a doctoral grant for E.W Nyaga grant from Université Paris Cité. We thank Professor Paulina Jaramillo (Carnegie Mellon University) for contributing to the purchase of the Clarity nodes. We recognise the Newton Fund Project in collaboration with University of Leicester, UK, and International Science Programme, Sweden, for facilitation of a BAM1020 and its operation at the University of Nairobi. We acknowledge the support of Moses Njeru, Mathias Mailu, Daniel Njoroge, and Saimon Bartilol from the Institute of Nuclear Science of the University of Nairobi. They were responsible for the operation and maintenance of the instruments. The authors declare no conflict of interest. Data used in this work is stored in the cloud by the Clarity sensor-nodes manufacturer and can be accessed via (<https://dash-board.clarity.io/sign-in>) upon request. We would also like to acknowledge the US embassy in Nairobi ([https://www.airnow.gov/international/us-embassies-and-consulates/#Kenya\\$Nairobi](https://www.airnow.gov/international/us-embassies-and-consulates/#Kenya$Nairobi)) for providing open access historic PM_{2.5} measurements that have been incorporated into our work.

Appendix A. Supplementary data

Supplementary data to this article can be found online at <https://doi.org/10.1016/j.apr.2025.102630>.

References

- Austin, E., Novoselov, I., Seto, E., Yost, M.G., 2015. Laboratory evaluation of the shinyei PPD42NS low-cost particulate matter sensor. *PLoS One* 10 (9), e0137789. <https://doi.org/10.1371/journal.pone.0137789>.
- Behera, S.N., Sharma, M., 2010. Reconstructing primary and secondary components of PM_{2.5} composition for an urban atmosphere. *Aerosol. Sci. Technol.* 44 (11), 983–992. <https://doi.org/10.1080/02786826.2010.504245>.
- Boiyo, R., Kumar, K.R., Zhao, T., 2018. Spatial variations and trends in AOD climatology over East Africa during 2002–2016: a comparative study using three satellite data sets. *Int. J. Climatol.* 38 (S1). <https://doi.org/10.1002/joc.5446>.

- Castells-Quintana, D., Wenban-Smith, H., 2020. Population dynamics, urbanisation without growth, and the rise of megacities. *J. Dev. Stud.* <https://www.tandfonline.com/doi/abs/10.1080/00220388.2019.1702160>.
- Chen, S.-L., Chang, S.-W., Chen, Y.-J., Chen, H.-L., 2021. Possible warming effect of fine particulate matter in the atmosphere. *Commun. Earth Environ.* 2 (1), 1–9. <https://doi.org/10.1038/s43247-021-00278-5>.
- Cordell, R.L., Panchal, R., Bernard, E., Gatari, M., Waiguru, E., Ng'ang'a, M., Nyang'aya, J., Ogot, M., Wilde, M.J., Wyche, K.P., Abayomi, A.A., Alani, R., Monks, P.S., Vande Hey, J.D., 2021. Volatile organic compound composition of urban air in Nairobi, Kenya and Lagos, Nigeria. *Atmosphere* 12 (10), 1329. <https://doi.org/10.3390/atmos12101329>.
- Crilley, L.R., Shaw, M., Pound, R., Kramer, L.J., Price, R., Young, S., Lewis, A.C., Pope, F.D., 2018. Evaluation of a low-cost optical particle counter (Alphasense OPC-N2) for ambient air monitoring. *Atmos. Meas. Tech.* 11 (2), 709–720. <https://doi.org/10.5194/amt-11-709-2018>.
- deSouza, P., Nthusi, V., Klopp, J., Shaw, B., Ho, W., Saffell, J., Jones, R., Ratti, C., 2017. A Nairobi experiment in using low cost air quality monitors. *Clean Air J.* 27 (2). <https://doi.org/10.17159/2410-972X/2017/v27n2a6>.
- Egondi, T., Muindi, K., Kyobutungi, C., Gatari, M., Rocklöv, J., 2016. Measuring exposure levels of inhalable airborne particles (PM 2.5) in two socially deprived areas of Nairobi, Kenya. *Environ. Res.* 148, 500–506. <https://doi.org/10.1016/j.enres.2016.03.018>.
- Elson, P., Sales De Andrade, E., Hattersley, R., Campbell, E., Dawson, A., May, R., Little, B., Pelley, C., Blay, B., Donkers, K., 2018. SciTools/cartopy: V0. 17.0. Zenodo. https://ui.adsabs.harvard.edu/abs/2018zenndo_1490296E/abstract.
- Fisher, S., Bellinger, D.C., Cropper, M.L., Kumar, P., Binagwaho, A., Koudenkoupo, J.B., Park, Y., Taghian, G., Landrigan, P.J., 2021. Air pollution and development in Africa: impacts on health, the economy, and human capital. *Lancet Planet. Health* 5 (10), e681–e688. [https://doi.org/10.1016/S2542-5196\(21\)00201-1](https://doi.org/10.1016/S2542-5196(21)00201-1).
- Gaita, S.M., Boman, J., Gatari, M.J., Pettersson, J.B.C., Janhäll, S., 2014. Source apportionment and seasonal variation of PM_{2.5} in a Sub-Saharan African city: Nairobi, Kenya. *Atmos. Chem. Phys.* 14 (18), 9977–9991. <https://doi.org/10.5194/acp-14-9977-2014>.
- Gatari, M.J., Boman, J., Wagner, A., 2009. Characterization of aerosol particles at an industrial background site in Nairobi, Kenya. *X Ray Spectrom.* 38 (1), 37–44. <https://doi.org/10.1002/xrs.1097>.
- Giordano, M.R., Malings, C., Pandis, S.N., Presto, A.A., McNeill, V.F., Westervelt, D.M., Beekmann, M., Subramanian, R., 2021. From low-cost sensors to high-quality data: a summary of challenges and best practices for effectively calibrating low-cost particulate matter mass sensors. *J. Aerosol Sci.* 158, 105833. <https://doi.org/10.1016/j.jaerosci.2021.105833>.
- Gobel, D., Schloesser, H., Pottberg, T., 2008. Met one instruments BAM-1020 beta attenuation mass monitor US-EPA PM2. 5 federal equivalent method field test results. The Air & Waste Management Association (A&WMA) Conference, Kansas City, MO 2 (3). <https://citeseerx.ist.psu.edu/document?repid=rep1&type=pdf&doi=88d61918ad5d5772fe78f624776f543f62d9f43>.
- Gonzalez, A., Boies, A., Swason, J., Kittelson, D., 2019. Field calibration of low-cost air pollution sensors. *Gases/In Situ Measurement/Instruments and Platforms*. <https://doi.org/10.5194/amt-2019-299>.
- Henne, S., Junkermann, W., Kariuki, J.M., Aseyo, J., Klausen, J., 2008. Mount Kenya global atmospheric watch station (MKN): installation and meteorological characterization. *J. Appl. Meteorol. Climatol.* 47 (11), 2946–2962. <https://doi.org/10.1175/2008AMC1834.1>.
- Jayaratne, R., Liu, X., Ahn, H.-K., Aslamud-Sakyi, A., Fisher, G., Gao, J., Mabon, A., Mazaheri, M., Mullins, B., Nyaku, M., Ristovski, Z., Scorgie, Y., Thai, P., Dunbabin, M., Morawska, L., 2020. Low-cost PM_{2.5} sensors: an assessment of their suitability for various applications. *Aerosol Air Qual. Res.* <https://doi.org/10.4209/aaqr.2018.10.0390>.
- Kalisa, W., Zhang, J., Igbawua, T., Henchiri, M., Mulinga, N., Nibagwire, D., Umuhoho, M., 2023. Spatial and temporal heterogeneity of air pollution in East Africa. *Sci. Total Environ.* 886, 163734. <https://doi.org/10.1016/j.scitotenv.2023.163734>.
- Kelly, K.E., Whitaker, J., Petty, A., Widmer, C., Dybwad, A., Sleeth, D., Martin, R., Butterfield, A., 2017. Ambient and laboratory evaluation of a low-cost particulate matter sensor. *Environ. Pollut.* 221, 491–500. <https://doi.org/10.1016/j.envpol.2016.12.039>.
- Kinney, P.L., Gichuru, M.G., Volavka-Close, N., Ngo, N., Ndiba, P.K., Law, A., Gachanja, A., Gaita, S.M., Chillrud, S.N., Sclar, E., 2011. Traffic impacts on PM2.5 air quality in Nairobi, Kenya. *Environ. Sci. Pol.* 14 (4), 369–378. <https://doi.org/10.1016/j.envsci.2011.02.005>.
- Kirago, L., Gatari, M.J., Gustafsson, Ö., Andersson, A., 2022. Black carbon emissions from traffic contribute substantially to air pollution in Nairobi, Kenya. *Commun. Earth Environ.* 3 (1), 74. <https://doi.org/10.1038/s43247-022-00400-1>.
- Lenschow, P., 2001. Some ideas about the sources of PM10. *Atmos. Environ.* 35, 23–33. [https://doi.org/10.1016/S1352-2310\(01\)00122-4](https://doi.org/10.1016/S1352-2310(01)00122-4).
- Malings, C., Tanzer, R., Hauryliuk, A., Kumar, S.P.N., Zimmerman, N., Kara, L.B., Presto, A.A., Subramanian, R., 2019. Development of a general calibration model and long-term performance evaluation of low-cost sensors for air pollutant gas monitoring. *Atmos. Meas. Tech.* 12 (2), 903–920. <https://doi.org/10.5194/amt-12-903-2019>.
- Malings, C., Tanzer, R., Hauryliuk, A., Saha, P.K., Robinson, A.L., Presto, A.A., Subramanian, R., 2020. Fine particle mass monitoring with low-cost sensors: corrections and long-term performance evaluation. *Aerosol. Sci. Technol.* 54 (2), 160–174. <https://doi.org/10.1080/02786826.2019.1623863>.
- Manshur, T., Luit, C., Avis, W.R., Bukachi, V., Gatari, M., Mulligan, J., Radcliffe, J., Singh, A., Waiguru, E., Wandera, A., 2023. A citizen science approach for air quality monitoring in a Kenyan informal development. *City and Environment Interactions* 19, 100105. <https://www.sciencedirect.com/science/article/pii/S259025202000077>.
- McFarlane, C., Raheja, G., Malings, C., Appoh, E.K.E., Hughes, A.F., Westervelt, D.M., 2021. Application of gaussian mixture regression for the correction of low cost PM_{2.5} monitoring data in Accra, Ghana. *ACS Earth Space Chem.* 5 (9), 2268–2279. <https://doi.org/10.1021/acsearthspacechem.1c00217>.
- Miech, J.A., Stanton, L., Gao, M., Micalizzi, P., Uebelherr, J., Herckes, P., Fraser, M.P., 2021. Calibration of low-cost NO₂ sensors through environmental factor correction. *Toxics* 9 (11). <https://doi.org/10.3390/toxics9110281>, Article 11.
- Mundi, K., Kimani-Murage, E., Egondi, T., Rocklov, J., Ng, N., 2016. Household air pollution: sources and exposure levels to fine particulate matter in Nairobi slums. *Toxics* 4 (3). <https://doi.org/10.3390/toxics4030012>, Article 3.
- Mutahi, A.W., Borgese, L., Marchesi, C., Gatari, M.J., Depero, L.E., 2021. Indoor and outdoor air quality for sustainable life: a case study of rural and urban settlements in poor neighbourhoods in Kenya. *Sustainability* 13 (4), 2417. <https://doi.org/10.3390/su13042417>.
- NCEI, 2024. Ncei. National Centers for Environmental Information (NCEI), 2024, December 6. <https://www.ncei.noaa.gov/access/search/data-search/global-hourly?bbox=-1.306,36.900,-1.356,36.950&pageNum=1&startDate=2021-01-01T00:00:00&endDate=2021-03-01T23:59:59>.
- Njeru, M.N., Mwangi, E., Gatari, M.J., Kaniu, M.I., Kanyeria, J., Raheja, G., Westervelt, D.M., 2024. First results from a calibrated network of low-cost PM_{2.5} monitors in Mombasa, Kenya show exceedance of healthy guidelines. *GeoHealth* 8 (9), e2024GH001049. <https://doi.org/10.1029/2024GH001049>.
- Nthusi, V., 2017. Nairobi air quality monitoring sensor network report—april 2017. <https://doi.org/10.13140/RG.2.2.10240.64009>.
- Okure, D., Ssematimba, J., Sserunjogi, R., Gracia, N.L., Soppelsa, M.E., Bainomugisha, E., 2022. Characterization of ambient air quality in selected urban areas in Uganda using low-cost sensing and measurement technologies. *Environ. Sci. Technol.* 56 (6), 3324–3339. <https://doi.org/10.1021/acs.est.1c01443>.
- Ouimet, J., Arnott, W.P., Laven, P., Whitwell, R., Radhakrishnan, N., Dhaniyala, S., Sandink, M., Tryner, J., Volckens, J., 2024. Fundamentals of low-cost aerosol sensor design and operation. *Aerosol. Sci. Technol.* <https://www.tandfonline.com/doi/abs/10.1080/02786826.2023.2285935>.
- Panda, U., Dey, S., Sharma, A., Singh, A., Reyes-Villegas, E., Darbyshire, E., Carbone, S., Das, T., Allan, J., McMiggans, G., Ravikrishna, R., Coe, H., Liu, P., Gunthe, S.S., 2025. Exploring the chemical composition and processes of submicron aerosols in Delhi using aerosol chemical speciation monitor driven factor analysis. *Sci. Rep.* 15 (1), 14383. <https://doi.org/10.1038/s41598-025-99245-9>.
- Pope, C.A., Dockery, D.W., 2006. Health effects of fine particulate air pollution: lines that connect. *J. Air Waste Manag. Assoc.* 56 (6), 709–742. <https://doi.org/10.1080/10473289.2006.10464485>.
- Pope, F.D., Gatari, M., Ng'ang'a, D., Poynter, A., Blake, R., 2018. Airborne particulate matter monitoring in Kenya using calibrated low-cost sensors. *Atmos. Chem. Phys.* 18 (20), 15403–15418. <https://doi.org/10.5194/acp-18-15403-2018>.
- Raheja, G., Nimo, J., Appoh, E.K.-E., Essien, B., Sunu, M., Nyante, J., Amegah, M., Quansah, R., Arku, R.E., Penn, S.L., Giordano, M.R., Zheng, Z., Jack, D., Chillrud, S., Amegah, K., Subramanian, R., Pinder, R., Appah-Sampong, E., Tetteh, E.N., et al., 2023. Low-cost sensor performance intercomparison, correction factor development, and 2+ years of ambient PM_{2.5} monitoring in Accra, Ghana. *Environ. Sci. Technol.* 57 (29), 10708–10720. <https://doi.org/10.1021/acs.est.2c09264>.
- Si, M., Xiong, Y., Du, S., Du, K., 2020. Evaluation and calibration of a low-cost particle sensor in ambient conditions using machine-learning methods. *Atmos. Meas. Tech.* 13 (4), 1693–1707. <https://doi.org/10.5194/amt-13-1693-2020>.
- Subramanian, R., Kagabo, A.S., Baharane, V., Guhirwa, S., Sindayigaya, C., Malings, C., Williams, N.J., Kalisa, E., Li, H., Adams, P., Robinson, A.L., DeWitt, H.L., Gasore, J., Jarillo, P., 2020. Air pollution in Kigali, Rwanda: spatial and temporal variability, source contributions, and the impact of car-free sundays. *Clean Air J* 30 (2).
- United Nations, 2018. Revision of World Urbanization Prospects. United Nations, New York, NY, USA, p. 799.
- WHO, W.H.O., 2021. WHO Global Air Quality Guidelines: Particulate Matter (PM_{2.5} and PM10), Ozone, Nitrogen Dioxide, Sulfur Dioxide and Carbon Monoxide. World Health Organization. <https://iris.who.int/handle/10665/345329>.
- Yadav, R., Sugha, A., Bhatti, M.S., Kansal, S.K., Sharma, S.K., Mandal, T.K., 2022. The role of particulate matter in reduced visibility and anionic composition of winter fog: a case study for Amritsar city. *RSC Adv.* 12 (18), 11104–11112. <https://doi.org/10.1039/D2RA00424K>.
- Yang, W., Seager, R., Cane, M.A., Lyon, B., 2015. The annual cycle of East African precipitation. *J. Clim.* 28 (6), 2385–2404. <https://journals.ametsoc.org/view/journals/clim/28/6/jcli-d-14-00484.1.xml>.
- Zaidan, M.A., Hossein Motlagh, N., Fung, P.L., Lu, D., Timonen, H., Kuula, J., Niemi, J.V., Tarkoma, S., Petaja, T., Kulmala, M., Hussein, T., 2020. Intelligent calibration and virtual sensing for integrated low-cost air quality sensors. *IEEE Sens. J.* 20 (22), 13638–13652. <https://doi.org/10.1109/JSEN.2020.3010316>.
- Zimmerman, N., Li, H.Z., Ellis, A., Hauryliuk, A., Robinson, E.S., Gu, P., Shah, R.U., Ye, Q., Snell, L., Subramanian, R., Robinson, A.L., Apte, J.S., Presto, A.A., 2020. Improving correlations between land use and air pollutant concentrations using wavelet analysis: insights from a low-cost sensor network. *Aerosol Air Qual. Res.* 20 (2), 314–328. <https://doi.org/10.4209/aaqr.2019.03.0124>.
- Zou, Y., Clark, J.D., May, A.A., 2021. Laboratory evaluation of the effects of particle size and composition on the performance of integrated devices containing Plantower particle sensors. *Aerosol. Sci. Technol.* 55 (7), 848–858. <https://doi.org/10.1080/02786826.2021.1905148>.